

See discussions, stats, and author profiles for this publication at: <https://www.researchgate.net/publication/229048703>

# Studies of Bitumen– Silica and Oil– Silica Interactions in Ionic Liquids

ARTICLE *in* ENERGY & FUELS · JANUARY 2011

Impact Factor: 2.79 · DOI: 10.1021/ef101404k

---

CITATIONS

20

---

READS

52

5 AUTHORS, INCLUDING:



[E. Manias](#)

Pennsylvania State University

134 PUBLICATIONS 5,804 CITATIONS

[SEE PROFILE](#)



[P. C. Painter](#)

Pennsylvania State University

161 PUBLICATIONS 3,188 CITATIONS

[SEE PROFILE](#)

## Studies of Bitumen–Silica and Oil–Silica Interactions in Ionic Liquids

Charles G. Hogshead, Evangelos Manias, Phillip Williams, Aron Lupinsky, and Paul Painter\*

Department of Materials Science and Engineering, and Department of Energy and Minerals Engineering,  
Pennsylvania State University, University Park, Pennsylvania 16802, United States

Received October 14, 2010. Revised Manuscript Received November 17, 2010

Previous work in this laboratory has shown that bitumen and oil can be readily separated from sand, using ionic liquids at ambient temperatures. To probe the mechanism underlying the relative ease of separation, atomic force microscopy (AFM) has been used to study interaction forces and adhesion between bitumen surfaces and a silica probe in the presence of liquid media. The energy of adhesion between bitumen samples obtained from both Canadian and U.S. oil sands are approximately an order of magnitude smaller in an ionic liquid medium than in aqueous solution. This behavior was traced to the ability of ionic liquids to form layered charge structures on surfaces. Although interactions between the silica probe and an aged crude oil sample could not be determined, because the probe adhesion to the oil film exceeded the force capacity of the AFM, thermodynamic considerations indicate that the energy of separation of silica from aged oil is also significantly smaller in an ionic liquid medium than in aqueous solution.

### Introduction

The separation and recovery of hydrocarbons from sand or other minerals is a critical problem in many industries, and it is crucial to the mitigation of environmental disasters, such as those associated with oil spills. For example, the separation of bitumen from Canadian oil sands requires significant amounts of energy and water and poses several environmental challenges.<sup>1–4</sup> Significant quantities of tar sands deposits can also be found in the western United States, notably Utah, but these are more difficult to process, because of their consolidated nature and the high viscosity of the bitumen.<sup>5,6</sup> Separating oil from sand that has been contaminated as a result of an spill—either accidental, as in the Exxon Valdez and Deepwater Horizon incidents, or as a deliberate act of war, as in Kuwait—also poses problems, because they do not completely remove the oil, are uneconomical because of energy requirements, or the chemicals used may pose unacceptable environmental concerns.<sup>7</sup>

A crucial factor in oil or bitumen separation from sand is the surface interactions between the components of the mixture. The literature that is concerned with the study of interaction forces and the thermodynamics of Canadian and Utah oil sands is particularly rich and deep. Our purpose is not to review this literature; we will only refer to papers that appear most relevant to the results that we will present here. In this regard, the work of Masliyah, Xu, and co-workers, using zeta potential distribution measurements and atomic force

microscopy (AFM), are particularly important.<sup>8–12</sup> (Much earlier work is also reviewed comprehensively in these papers.) These authors measured the repulsive long-range forces between bitumen and silica particles,<sup>9</sup> bitumen and clays, and bitumen and fines.<sup>10,11</sup> As might be expected, these forces are electrostatic in origin. They are weakest at low pH but increase significantly at higher pH.<sup>9</sup> As with other colloidal systems, the range of these forces decreases as the electrolyte concentration increases. Increasing the temperature also increases the repulsive forces, while adhesive forces decrease significantly as the temperature is increased, becoming very small for clay–bitumen interactions at temperatures above 32–35 °C.<sup>12</sup>

Several authors have also discussed thermodynamic aspects of the bitumen/sand interface and the work of separation.<sup>5,13–16</sup> In a seminal paper, Leja and Bowman<sup>13</sup> described the factors that contribute to the free energy of the interface and observed that, in most treatments of oil displacement from sand, it has been common practice to consider surface work only, expressed in terms of the surface tension of the various components in contact with each other. They pointed out that changes in interfacial area also play a significant role in oil or bitumen displacement from mineral surfaces. Schramm and Smith<sup>14</sup> also discussed the thermodynamic forces at play in the separation process, with a particular emphasis on the importance of surfactants. Various authors subsequently have made important measurements of the surface tension of bitumen<sup>17–22</sup> and the wettability of the sand particles.<sup>23–25</sup>

\*Author to whom correspondence should be addressed. E-mail: painter@matse.psu.edu.

(1) *Canada's Oil Sands—Opportunities and Challenges to 2015: An Update—June 2006*, National Energy Board, 2006. (Available via the Internet at <http://www.neb.gc.ca/clf-nsi/rnrgynfntn/nrgyrprt/lsnd/lsnd-eng.html>.)

(2) Allen, E. W. *J. Environ. Eng. Sci.* **2008**, *7*, 123–138.

(3) Allen, E. W. *J. Environ. Eng. Sci.* **2008**, *7*, 499–524.

(4) Masliyah, J.; Zhou, Z.; Xu, Z.; Czarnecki, J.; Hamza, H. *Can. J. Chem. Eng.* **2004**, *82*, 628–654.

(5) Drelich, J. *Miner. Metall. Process.* **2008**, *25*, 1–12.

(6) Miller, J. D.; Misra, M. *Fuel Process. Technol.* **1982**, *6*, 27–59.

(7) Veil, J. A. *J. Energy Resour. Technol.* **2003**, *125*, 238–248.

(8) Liu, J.; Zhou, Z.; Xu, Z.; Masliyah, J. *J. Colloid Interface Sci.* **2002**, *252*, 409–418.

(9) Liu, J.; Xu, Z.; Masliyah, J. *Langmuir* **2003**, *19*, 3911–3920.

(10) Liu, J.; Xu, Z.; Masliyah, J. *Can. J. Chem. Eng.* **2004**, *82*, 655–666.

(11) Liu, J.; Xu, Z.; Masliyah, J. *J. Colloid Interface Sci.* **2005**, *287*, 507–520.

(12) Long, J.; Xu, Z.; Masliyah, J. *Energy Fuels* **2005**, *19*, 1440–1446.

(13) Leja, J.; Bowman, C. W. *Can. J. Chem. Eng.* **1968**, *46*, 479–481.

(14) Schramm, L. L.; Smith, R. G. *Colloids Surf.* **1985**, *14*, 67–85.

(15) Wu, X. A.; Czarnecki, J. *Energy Fuels* **2005**, *19*, 1353–1359.

(16) Czarnecki, J.; Radoev, B.; Schramm, L. L.; Slavchev, R. *Adv. Colloid Interface Sci.* **2005**, *114–115*, 53–60.

(17) Vargha-Butler, E. I.; Zubovits, T. K.; Budziak, C. J.; Neumann, A. W. *Energy Fuels* **1988**, *2*, 653–656.

Ionic liquids (ILs) consist of organic cations associated with various anions that melt at or below 100 °C. Many ILs are liquids at room temperature, as a result of their asymmetric structures. They have outstanding chemical and thermal stability, are largely nonflammable, and have an almost negligible vapor pressure.<sup>26–28</sup> Accordingly, they are now being considered as attractive solvents for many chemical processes.<sup>29</sup> In this regard, we have recently found that bitumen can be cleanly separated from medium- and low-grade Canadian oil sands at ambient temperatures using appropriate ILs.<sup>30,31</sup> The method can also be used to separate bitumen from Utah tar sands<sup>32</sup> or aged oil from contaminated beach sand.<sup>33</sup> Essentially, this process involves the formation of a multiphase system obtained by simply mixing the oil- or tar-coated sands or minerals with an IL and a hydrophobic organic solvent at ambient temperatures (~25 °C). The bitumen or oil is detached from the sand in this process and forms an organic layer on the surface of the mixture that can be easily removed by decantation or other means. The organic solvent serves to reduce the viscosity of the bitumen or other heavy oil and sharpen the phase boundaries between the phase-separated components, thus facilitating separation. However, the work reported so far has focused on simply reporting what we consider to be intriguing and important observations. Although it seems likely that electrostatic interactions between the mineral surfaces and ILs are a driving force for the detachment of largely hydrophobic hydrocarbons, a study of these interactions was not part of these prior preliminary works. Here, we extend these initial studies by presenting results obtained using AFM and contact angle measurements to probe the interactions between bitumen and silica in the presence of an IL. Oil/silica interactions could not be studied by this method, for reasons described in the text; however, some insight could be gained through contact angle measurements.

### Materials and Methods

The bitumen samples used in this study were extracted from medium-grade Canadian oil sands and Utah tar sands. The Canadian oil sand was obtained from the Alberta Research Council, while the Utah tar sand sample was provided by the Utah Geological Survey and obtained from the Asphalt Ridge

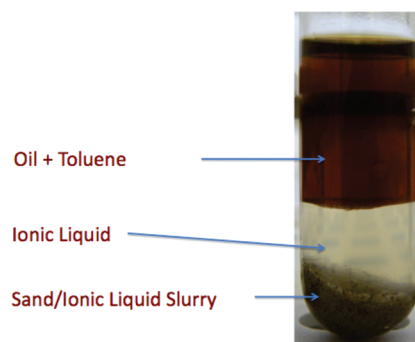


**Figure 1.** Photograph showing the phases formed by mixing an oil/sand mixture with 1-butyl-2,3-dimethyl-imidazolium borontetrafluoride ([bmim][BF<sub>4</sub>]) and toluene in the proportions 1:2:3 at room temperature.

Area of Uintah County, Utah (AF Hole No. 1, 44–54 ft, Box 3). The sand used in this study was obtained from a beach on Hilton Head Island, South Carolina. A sample of Pennsylvania crude oil was purchased from ONTA, Inc. A sample of oil-contaminated sand was prepared by simply mixing beach sand with oil to give a mixture that was 15% oil (by weight). This sample was “aged” by heating under vacuum at 75 °C for three days.

The bitumen or oil was separated from sand using the IL 1-butyl-2,3-dimethyl-imidazolium tetrafluoroborate ([bmim][BF<sub>4</sub>]), following the procedure described in previous work.<sup>30,31</sup> Essentially, the oil sand, the IL, and a nonpolar solvent (in this case, toluene) are simply stirred together in the proportions 1:2:3 at room temperature. Upon being allowed to stand, the components phase-separate into a sand/IL slurry, an IL layer, and a hydrocarbon layer. Bitumen/oil sand separations have been illustrated in previous studies,<sup>30–32</sup> and Figure 1 demonstrates that oil-contaminated sand can be separated just as easily, using this method. Different relative proportions oil sands or oil/mineral mixtures to IL to nonpolar solvent can be used to obtain a separation, the proportions 1:2:3 being chosen for this study to allow a clear visualization of the phase separated domains and to facilitate laboratory separations.

The infrared spectra of the bitumen or oil obtained by this extraction showed no evidence of the presence of residual sand or clay fines. Although we have used other ILs and IL/water mixtures successfully in recent work, this particular IL was the one chosen in our original studies and was therefore used here. The IL was purchased from Sigma–Aldrich and used as received.

Mechanical-grade, single-side-polished, *n*-type silicon (111) wafers were purchased from University Wafer. Silica spheres, purchased from SiliCycle, were used for all AFM experiments and possessed well-defined spherical shapes and a diameter of ~40 μm. V-shaped contact AFM cantilevers were purchased from MikroMasch (cantilever length = 290 μm; nominal spring constant of  $k = 0.12$  N/m; nominal resonance frequency = 12 kHz).

Bitumen films from Alberta tar sands and Utah oil sands were spin-cast from toluene solution (10 mg of bitumen per 1 mL of toluene) using a WS-400–6NPP-Lite spin-caster (Laurell Technologies Corporation). The films were spin-cast on clean silicon substrates (2 cm × 2 cm) using a three-step procedure. The first step lasted for 10 s at 100 rpm, the second step was for 20 s at 3000 rpm, and the final step lasted for 60 s at 5000 rpm. After the spin coating procedure, the films were dried in a fume hood for ~12 h under ambient conditions. The

- (18) Drelich, J.; Miller, J. D. *Fuel* **1994**, 73, 1504–1510.
- (19) Drelich, J.; Bukka, K.; Miller, J. D.; Hanson, V. *Energy Fuels* **1994**, 8, 700–704.
- (20) Drelich, J.; Lelinski, D.; Miller, J. D. *Colloids Surf., A* **1996**, 116, 211–223.
- (21) Schramm, L. L.; Stasiuk, E. N.; Turner, D. *Fuel Process. Technol.* **2003**, 80, 101–118.
- (22) Wu, X. A.; Czarnecki, J. *Energy Fuels* **2005**, 19, 1353–1359.
- (23) Darcovich, K.; Kotlyar, L. S.; Tse, W. C.; Ripmeester, J. A.; Capes, C. E.; Sparks, B. D. *Energy Fuels* **1989**, 3, 386–391.
- (24) Dang-Vu, T.; Jha, R.; Wu, S.-Y.; Tannant, D. D.; Masliyah, J.; Xu, Z. *Energy Fuels* **2009**, 23, 2628–2636.
- (25) Dang-Vu, T.; Jha, R.; Wu, S.-Y.; Tannant, D. D.; Masliyah, J.; Xu, Z. *Colloids Surf., A* **2009**, 337, 80–90.
- (26) Welton, T. *Chem. Rev.* **1999**, 99, 2071–2083.
- (27) Giernoth, R. *Top. Curr. Chem.* **2007**, 276, 1–23.
- (28) Weingartner, W. *Angew. Chem., Int. Ed.* **2008**, 47, 654–670.
- (29) Plechkova, N. V.; Seddon, K. R. *Chem. Soc. Rev.* **2008**, 37, 123–150.
- (30) Painter, P.; Williams, P.; Mannebach, E. *Energy Fuels* **2010**, 24, 1094–1098.
- (31) Williams, P.; Lupinsky, A.; Painter, P. C. *Energy Fuels* **2010**, 24, 2172–2173.
- (32) Painter, P.; Williams, P.; Lupinsky, A. *Energy Fuels* **2010**, 24, 5081–5088.
- (33) Painter, P.; Williams, P.; Lupinsky, A.; Klima, M. Unpublished work.

bitumen films were then copiously rinsed with deionized (DI) water and dried with a steady argon stream prior to use.

Pennsylvania crude oil was spin-cast directly (no solvent added) on clean silicon substrates also using a three-step procedure. The first step lasted for 10 s at 100 rpm, the second step was for 20 s at 2000 rpm, and the final step lasted for 60 s at 8000 rpm. After the spin coating procedure, the films were dried under vacuum at 75 °C for 72 h. The oil films were then rinsed with DI water and dried with a steady argon stream prior to use.

The sessile DI water (18 M $\Omega$  cm) contact angle and the sessile ionic liquid [bmim][BF<sub>4</sub>] contact angle were measured under ambient conditions for the bitumen films and the Pennsylvania crude oil films using a custom, side-mounted QX5 computer microscope set at 60X magnification. The contact angles were determined using software based on active contours<sup>34</sup> and the average contact angle from five, 5- $\mu$ L drops is reported. The contact angle measurements were conducted both before and after the AFM experiments, to ensure that the film had neither detached from the silicon substrate nor been appreciably damaged during the AFM study.

AFM force–distance measurements were conducted at room temperature on the bitumen films, on the Pennsylvania crude oil films, and on ultraviolet/ozone (UVO)-treated silicon wafers in both 1 mM KCl aqueous solution and in the ionic liquid [bmim][BF<sub>4</sub>], using a Molecular Imaging PicoSPM atomic force microscope. The spring constant of the silica-bearing cantilevers was measured, allowing for accurate determination of the AFM force (in the nano Newton (nN) range) by the measured cantilever deflection during force–distance experiments. A total of 100 force–distance curves (10 curves at 10 different spots) were collected for each system and the average adhesion is reported. For force–distance measurements obtained in aqueous solution, each approach/retraction cycle was collected over a duration of 2 s. For force–distance measurements obtained in the IL, each approach/retraction cycle was collected over a duration of 60 s, to eliminate any hydrodynamic drag forces experienced by the cantilever. Drag forces are rather strong here, as a result of the high viscosity of the ionic liquid and the low spring constant of the cantilever. It should be noted that hydrodynamic drag affects the “zero” force background (i.e., gives rise to an apparent force while the tip moves without being in contact with the sample surface), whereas the measured adhesion energies and repulsive forces were markedly unaffected (i.e., were independent of the approach/retraction rate for all measurements). In both the aqueous solution and the IL, there was no dwell time for the probe on the surface; instead, the cantilever was always positively deflected by  $\sim 3$  nN (compression force). Prior to the acquisition of the force–distance curves, all systems were allowed to equilibrate for  $\sim 1$  h.

The V-shaped cantilevers utilized for all of the AFM force–distance experiments in this study were modified by attaching a colloidal silica sphere to the end of the cantilever, using Aremco-Bond 2300 high-performance epoxy. The diameters of the colloidal probes were determined by scanning electron microscopy (SEM) (FEI Quanta 200 ESEM) and were in the range of 38–43  $\mu$ m. A micrograph of the probe is shown in Figure 2. Using an optical microscope, the colloidal probe was checked after each experiment to ensure that the

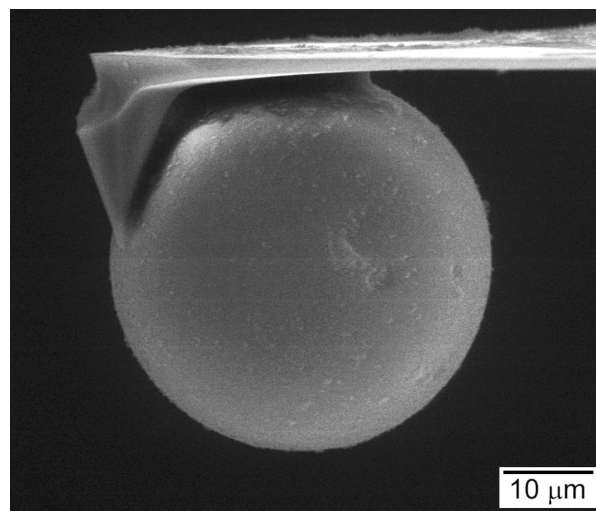


**Figure 2.** Scanning electron microscopy (SEM) photomicrograph of the silica colloidal probe attached on the AFM tip (diameter of sphere = 43.6  $\mu$ m, viz, a contact area of 1  $\mu$ m<sup>2</sup>), facilitating the measurement of surface forces, rather than the AFM-typical atomic forces measured by sharp AFM tips.

sphere remained properly attached. Because of the variation in spring constants between AFM cantilevers, the spring constant for each colloidal probe was measured by determining the resonance frequency of the cantilever before and after the addition of the silica sphere.<sup>35</sup> The spring constants were determined to vary from 0.03 N/m to 0.05 N/m, which is within the tolerances provided by the manufacturer. Similarly, because of the variation in the diameters of the attached silica spheres, all calculated adhesion energies were normalized by the contact area of the colloidal probe, determined by SEM, using the Johnson–Kendall–Roberts (JKR) theory.<sup>36–38</sup> The calculated contact areas varied from 0.94  $\mu$ m<sup>2</sup> to 1.17  $\mu$ m<sup>2</sup>. Prior to force–distance experiments for each surface, the silica colloidal probe was exposed to a UVO treatment to remove organic contaminants and was then rinsed with DI water. The UVO treatment was conducted at 60 °C for 5 min, and the colloidal probes were subsequently incubated in the UVO chamber for an additional 30 min.

## Results and Discussion

**Adhesion Energy Studies by AFM.** The AFM experiments involved direct force measurements between a bitumen surface and an extended silica probe (40- $\mu$ m sphere), mounted on the apex of a soft-contact mode AFM cantilever, while both are immersed in a solvent. It should be emphasized at the outset that

(a) these are *surface forces*, due to the silicon-sphere probe affording a 1  $\mu$ m<sup>2</sup> (1000 nm<sup>2</sup>) contact area, rather than *atomic forces*, as typically measured by AFM with sharp tips at a contact area of 10–50 nm<sup>2</sup>; and

(b) these surface forces are determined by the combination of interfacial surface energies between the three materials

(35) Cleveland, J. P.; Manne, S.; Bocek, D.; Hansma, P. K. *Rev. Sci. Instrum.* **1993**, *64*, 403–405.

(36) Johnson, K. L.; Kendall, K.; Roberts, A. D. *Proc. R. Soc. London, Ser. A* **1971**, *324*, 301–313.

(37) Israelachvili, J. *Intermolecular and Surface Forces*, Second ed.; Academic Press: New York, 1992.

(38) Noy, A.; Vezennov, D. V.; Lieber, C. M. *Annu. Rev. Mater. Sci.* **1997**, *27*, 381–421.

(34) Stalder, A. F.; Kulik, G.; Sage, D.; Barbieri, L.; Hoffman, P. *Colloids Surf., A* **2006**, *286*, 92–103.



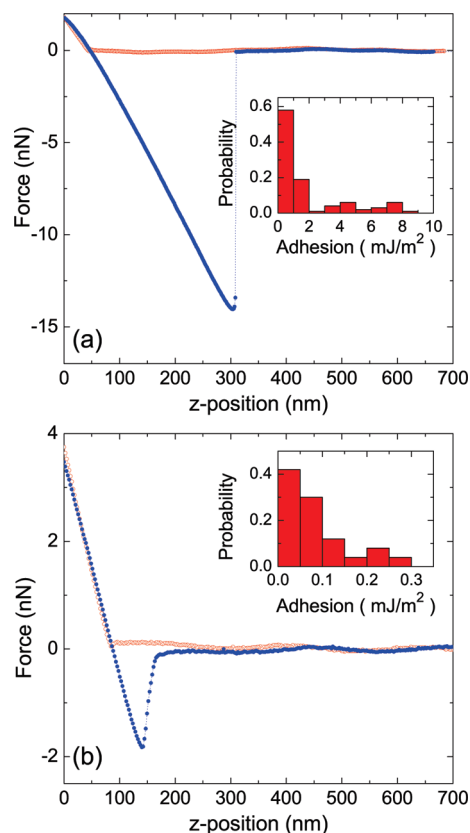


**Figure 3.** (a) Representative force–distance approach (red circles) and retraction (blue circles) curves for the bitumen film from Utah oil sands collected in a 1 mM KCl aqueous solution. Inset shows the adhesion histogram. (b) Representative force–distance approach (red circles) and retraction (blue circles) curves for the bitumen film from Utah oil sands collected in the ionic liquid (IL). Inset shows the adhesion histogram.

and, thus, primarily reflect the relative strength of surface–solvent and probe–solvent interactions, compared to the surface–probe interactions. (These last interactions are typically measured if the same experiment were conducted in air or, better, under vacuum.) Accordingly, the measured adhesion energies, in a first approximation,<sup>37,39</sup> correspond to the interaction energy of materials 1 and 2 immersed in a liquid 3 ( $w_{132} = \gamma_{13} + \gamma_{23} - \gamma_{12}$ , vide infra, eq 1, considered in a later section on contact angle measurements; a much more detailed discussion can be found in ref. 39).

For the bitumen obtained from Utah tar sands, the adhesion energy distribution and a representative force–distance curve obtained in a 1 mM KCl aqueous solution are shown in Figure 3A, whereas those obtained in the presence of the IL [bmim][BF<sub>4</sub>] are shown in Figure 3B. The force–distance curves collected both in the aqueous solution and in the IL appear similar on the approach of the silica probe to the bitumen surface, reflecting mostly repulsive interaction forces, similar to those observed in previous studies.<sup>9,11</sup> Both in aqueous solution and in the IL, there is a very small “jump-to-contact” (<0.1 nN), where the solvent-mediated attraction between the colloidal probe and the bitumen film exceeds the spring constant of the cantilever. Upon compression up to a normal load of 3 nN, the cantilever seems to experience all of the measurable deflection (i.e., we do not

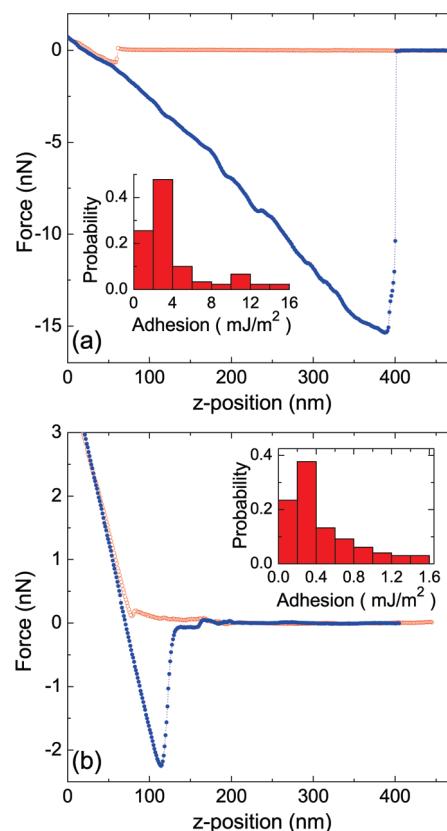


**Figure 4.** (A) Representative force–distance approach (red circles) and retraction (blue circles) curves for the bitumen film from Alberta tar sands collected in the 1 mM KCl aqueous solution. Inset shows the adhesion histogram. (B) Representative force–distance approach (red circles) and retraction (blue circles) curves for the bitumen film from Alberta tar sands collected in the IL. Inset shows the adhesion histogram.

observe any compression of the film). This was achieved by the combination of very soft cantilevers, allowing for very low compression loads (the spring constants of the contact-mode cantilevers used here are much smaller than the moduli of the bitumen films) and the use of a micrometer-sized silica probe, allowing for very low tip-applied pressures on the sample surface (due to a large contact area, 2 orders of magnitude larger than typical AFM tips).

In contrast to the forces measured on approach, the withdrawal curves measured in aqueous solution are significantly different than those measured in the IL. In aqueous solution, the average adhesion energy was determined to be 2.0 mJ/m<sup>2</sup>, whereas, in the IL, the average adhesion energy is only a fraction of this value (~0.1 mJ/m<sup>2</sup>). Accordingly, the average pull-off force is 14 nN in aqueous solution but only 2 nN in the IL. Both adhesion peaks are smooth and there is no evidence of any appreciable sample deformation upon tip retraction: the probe appeared to detach or separate from the films cleanly, indicating only physisorption between the probe and the surfaces.

The adhesion energy distributions and a representative force–distance curve obtained for the bitumen obtained from the Alberta oil sand sample in 1 mM KCl aqueous solution are shown in Figure 4A, while those obtained in the presence of the [bmim][BF<sub>4</sub>] IL are shown in Figure 4B. The two approach curves appear qualitatively similar, but in the aqueous solution, there is a definitive jump-to-contact of ~0.7 nN (on average), compared to a jump-to-contact of

(39) van Oss, C. J.; Chaudhury, M. K.; Good, R. J. *Chem. Rev.* **1988**, *88*, 927–941.

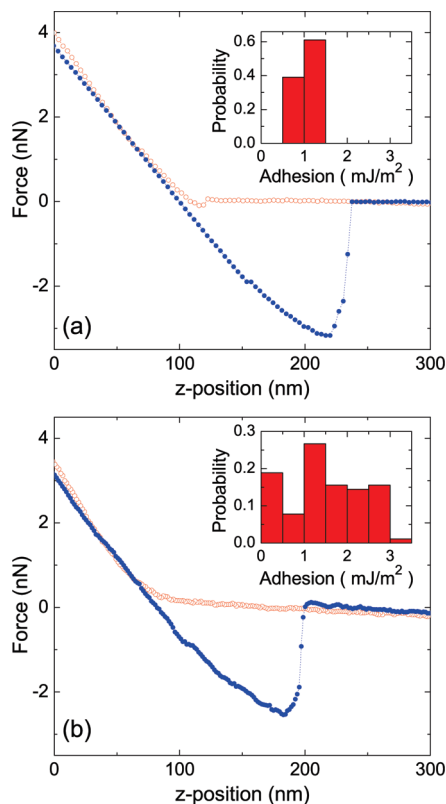


**Figure 5.** (A) Representative force–distance approach (red circles) and retraction (blue circles) curves for the bare silicon wafer collected in the 1 mM KCl aqueous solution. Inset shows the adhesion histogram. (B) Representative force–distance approach (red circles) and retraction (blue circles) curves for the bare silicon wafer collected in the IL. Inset shows the adhesion histogram.

~0.1 nN in the IL (for the same cantilever/probe); this behavior indicates longer-range and/or stronger silica–bitumen attraction in water than in the IL, which probably originates from differences in the charge density near the bitumen surface in the two liquids (vide infra). The withdrawal forces seem to be very different when comparing the two solutions. The average pull-off force in aqueous solution is 15 nN, whereas, in the IL, it is only 2 nN; the corresponding solvent-mediated silica/bitumen adhesion energies are 4.2 mJ/m<sup>2</sup> for water/KCl, and only 0.5 mJ/m<sup>2</sup> for the IL. All these values show an excellent correlation to those observed for the Utah sample. Specifically, the silica pull-off forces are very similar for the two bitumens and the relative adhesion energy decreases by 1 order of magnitude when aqueous KCl solutions are replaced by IL. However, the values of adhesion are higher for the Alberta bitumen films both in the aqueous solution and in the IL. As with the Utah bitumen, we do not observe any film compression upon approach, but the withdrawal curves collected in aqueous solution manifest a jaggedness in the adhesion force peak (i.e., in the aqueous medium, there evidently exist inhomogeneities and possibly structural changes that are coupled with surface adhesion, whereas in the IL, the withdrawal curve is devoid of any features and is consistent with forces purely due to surface adhesion). The pull-off forces obtained here are a factor of ~2 lower than those obtained by Masliyah et al. (using silica microspheres and 1 mM KCl aqueous solution<sup>9,11</sup>) when accounting for the differences in the diameters of the microspheres. However, considering the different source for the

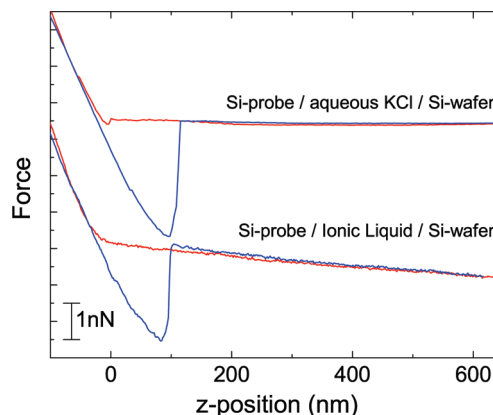


**Figure 6.** Force–distance atomic force microscopy (AFM) curves of a colloidal silica probe and a silicon-surface immersed in 1 mM KCl aqueous solution and in [bmim][BF<sub>4</sub>] IL (the lines are shifted for the sake of clarity, and the long-range approach forces are contrasted, in water versus in IL). There are no measurable long-range forces in aqueous KCl, whereas there is a systematic attraction in IL, acting over hundreds of nanometers above the silicon-wafer surface.

bitumen in those studies, the agreement in the measured pull-off forces is certainly very reasonable.

To gain further insight into the different effect of the two liquid media on the surface forces and adhesion, control experiments were performed by measuring the forces between the same silica probe and a UVO-treated silicon wafer immersed in the same two media (i.e., in aqueous KCl solution and in [bmim][BF<sub>4</sub>] ionic liquid, Figure 5). Upon approach, there is a small but reproducible jump-to-contact of ~0.1 nN for aqueous KCl, while there is none in the IL, presumably as a result of a larger screening of electrostatic forces in an IL medium. Despite the slightly higher average pull-off force in the aqueous solution (3 nN, compared to 2.5 nN in IL), the measured average adhesion energies are 1.0 mJ/m<sup>2</sup> for aqueous KCl and 1.5 mJ/m<sup>2</sup> for the IL, showing a reversal of the adhesion strength, compared to what was observed for the two bitumen systems (i.e., here, there is a 50% higher silicon-probe/medium/silicon-surface adhesion in the IL, compared to aqueous KCl solutions). In contrast, both bitumen samples showed a 10-fold decrease in adhesion in the presence of the IL.

Some clues on the origin of this adhesion reversal can be found by an examination of the shape of the approach and withdrawal curve shown in Figure 5. The latter “maps out” the adhesive forces while the probe and surface are in contact, whereas the former reflects the long-range interactions well before the probe comes in contact with the surface. Focusing first on the approach curves in Figure 6, we observe a long-range attraction of the silicon colloidal-sphere probe when immersed in the IL, whereas there are no apparent long-range forces in aqueous KCl. This attractive force is acting on the silica probe over several hundreds of nanometers above the surface and therefore cannot possibly be attributed to atomic forces (van der Waals or electrostatic). We suggest that this is because ILs behave very differently at surfaces and charged interfaces than small ions in dilute solutions, forming alternating, discrete, solvation layers of ions.<sup>40–42</sup> This physical origin is in concert with the observed force magnitude (in the range of 1 nN for a 40-μm-diameter

(40) Atkin, R.; Warr, G. G. *J. Phys. Chem. C* **2007**, *111*, 5162–5168.

**Table 1. Results of Contact Angle Measurements**

surface	Water Contact Angle		IL Contact Angle
	Before AFM Expt	After AFM Expt	After AFM Expt
bitumen from Utah Oil Sands	89°	88°	64°
bitumen from Alberta Tar Sands	90°	89°	63°
aged crude oil sample		90°	73°

colloidal particle), and it also explains the absence of this force in aqueous media, where ion diffusivities are much higher (due to the lower viscosity of water) and the association energy of ions is much lower (due to the high permittivity of water).<sup>43–45</sup> In addition, charge layering would explain the features observed in the in-contact part of the withdrawal curves, which display some jaggedness in the force when collected in the IL, but are smooth for aqueous KCl. This behavior strongly indicates charge-layer restructuring leading to electrostatic force inhomogeneities. The observed adhesive force fluctuations cannot be attributed to sample deformation (the modulus of silicon is too high), nor can they be caused by any appreciable structural inhomogeneity within the silicon wafer. Because of this, and also because of the high concentration of electrolyte in the IL-mediated studies, the use of DeJaguin–Landau–Verwey–Overby (DLVO) theory to interpret and rationalize our observations, as in other AFM studies of interactions between bitumen and silica,<sup>9–12</sup> is inapplicable here.

Finally, we also attempted to make measurements on a sample of a crude oil “aged” at 75 °C under vacuum for 3 days. The adhesion was so high—both in 1 mM KCl aqueous solution and in the IL—that it could not be measured. The probe never detached from the film for the cantilevers used in this study and the sphere was eventually ripped off the cantilever (i.e., the adhesion was orders of magnitude higher for aged crude oil than in the bitumen samples studied above). Evidently, the crude oil films acted as a “glue”, most likely because of the low-molecular-weight species present in the film and, hence, its lower modulus; even though it could not be established whether the probe (colloidal sphere) was resting on the surface of the film or if it penetrated the film and was wetted by the crude oil (as indicated by the very long ranged surface deformation, in sharp contrast to the typical surface forces that we observed above). However, data on the surface adhesion was obtained using contact angle measurements, determined before and after the AFM experiments. These data are summarized in Table 1 and are considered in a later section.

**Distribution of AFM Adhesion Energies.** One of the aspects of the adhesion surface forces measured by AFM that was not discussed previously is related to the distribution of the measured adhesion energy. The probability histograms of adhesion energy provided with the force–distance curves

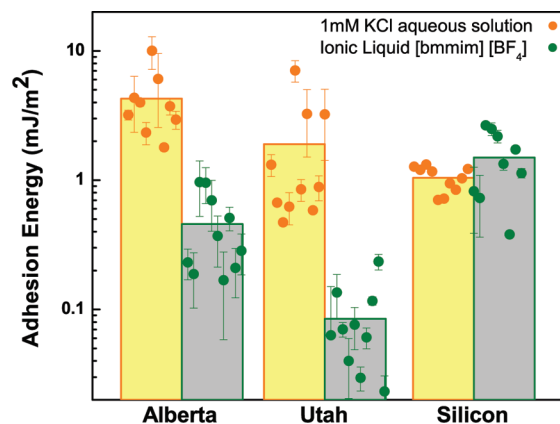


**Figure 7.** Comparison of the adhesion energies in both the aqueous solution and in the IL for the bitumen from Alberta tar sands, the bitumen from Utah oil sands, and the bare silicon control surface. The symbols and error bars depict measurements from different/independent spots on each surface; for each spot, the symbols provide the average adhesion value and the error bars depict the respective adhesion deviation around the average. The histogram bars depict the average adhesion energy for each system.

(insets in Figures 3–5) are rather broad in all cases, except for the silica-probe/aqueous-KCl/silicon-surface system (Figure 5A). A better depiction of the adhesion data is shown in Figure 7, where the symbols (solid circles) depict the average for different spots on each surface (10 force–distance measurements were made at each spot), the error bars depict the distribution of adhesion energies at each of these spots, and the histogram heights depict the average adhesion energy for each system (averaged over all spots and all force–distance curves).

It is evident from Figure 7 that the distribution of measured adhesions is much broader for the two bitumen samples than for the silicon. This behavior is intuitively expected, considering the structural inhomogeneities of bitumen systems,<sup>46</sup> compared to the silicon wafer, which, in turn, are expected to give rise to spatial variations in the AFM-probed atomic and surface forces; in fact, bitumen structural inhomogeneities have been shown<sup>46</sup> to be substantially larger than what is typically needed<sup>47–49</sup> for AFM to manifest large variations in adhesion energy across different spots on the surface. In addition, it can be seen that the distribution of the measured adhesion energies is broader in the presence of the IL, compared to the aqueous KCl for all three surfaces. This behavior most probably reflects the higher tendency for charge layering on the surfaces when immersed in the IL, compared to the aqueous KCl medium.

**Thermodynamic Considerations.** The results presented above clearly demonstrate that the forces of adhesion between bitumen films and a silica probe are significantly smaller in the presence of ILs than in aqueous solution. The fact that it would be easier to detach bitumen from a silica surface in the presence of ILs, relative to water, can also be demonstrated by some crude thermodynamic considerations. Neglecting changes in contact area (which, as Leja and

(41) Lauw, Y.; Horne, M. D.; Rodopoulos, T.; Leermakers, F. A. *Phys. Rev. Lett.* **2009**, *103*, 117801.

(42) Min, Y.; Akbulut, M.; Sangoro, J. R.; Kremer, F.; Prud'homme, R. K.; Israelachvili, J. *J. Phys. Chem. C* **2009**, *113*, 16445–16449.

(43) Lu, Z.; Polizos, G.; Macdonald, D. D.; Manias, E. *J. Electrochem. Soc.* **2008**, *155*, B163–B171.

(44) Lu, Z.; Lanagan, M.; Manias, E.; Macdonald, D. D. *J. Phys. Chem. B* **2009**, *113*, 13551–13559.

(45) Lu, Z.; Manias, E.; Macdonald, D. D.; Lanagan, M. *J. Phys. Chem. A* **2009**, *113*, 12207–12214.

(46) Drelich, J.; Long, J.; Yeung, A. *Can. J. Chem. Eng.* **2007**, *85*, 625–634.

(47) Efimenko, K.; Rackaitis, M.; Manias, E.; Vaziri, A.; Mahadevan, L.; Genzer, J. *Nat. Mater.* **2005**, *4*, 293–297.

(48) Efimenko, K.; Crowe, J. A.; Manias, E.; Schwark, D. W.; Fischer, D. A.; Genzer, J. *Polymer* **2005**, *49*, 9329–9341.

(49) Strawhecker, K.; Manias, E. *Macromolecules* **2001**, *34*, 8475–8482.

Bowman<sup>13</sup> noted many years ago, would favor detachment), we can write the following expression for the work of adhesion<sup>37,39</sup> ( $w_{b/w/s}$ ), which could also be called the work of separation, between bitumen (b) and silica (s) immersed in an aqueous medium (w), as

$$w_{b/w/s} = \gamma_{b/w} + \gamma_{s/w} - \gamma_{b/s} \quad (1)$$

The surface energies (per unit area) or surface tensions  $\gamma_{b/w}$ ,  $\gamma_{s/w}$ , and  $\gamma_{b/s}$  are for the bitumen/water, silica/water and bitumen/silica interfaces, respectively. Although important insights into wetting have been made through measurements of contact angles of bitumen on silica surfaces in aqueous solutions, as mentioned above, the use of eq 1 is limited by the problem of measuring solid/liquid interfacial tensions. However, we can compare the work of separation in two different liquids. Using the subscript “il” to designate measurements in an ionic liquid, we can write

$$w_{b/il/s} = \gamma_{b/il} + \gamma_{s/il} - \gamma_{b/s} \quad (2)$$

Subtracting eq 2 from eq 1 yields

$$w_{b/w/s} - w_{b/il/s} = (\gamma_{b/w} - \gamma_{b/il}) - (\gamma_{s/w} - \gamma_{s/il}) \quad (3)$$

This eliminates the  $\gamma_{b/s}$  term. The other surface terms can be expressed in terms of contact angle measurements, using Young’s equation.<sup>50</sup> Take the first term in parentheses in eq 3:

$$\gamma_{b/w} = \gamma_b - \gamma_w \cos \theta_{b/w} \quad (4)$$

$$\gamma_{b/il} = \gamma_b - \gamma_{il} \cos \theta_{b/il} \quad (5)$$

where  $\gamma_b$ ,  $\gamma_w$ , and  $\gamma_{il}$  are surface energies of bitumen, water, and the IL in contact with air, respectively. The contact angles  $\theta_{b/w}$  and  $\theta_{b/il}$  are close to 90° and 64°, respectively (see Table 1). The surface tension of [bmmim][BF<sub>4</sub>] has not been measured, but a very similar imidazolium IL, 1-butyl-2,3-dimethyl-imidazolium tetrafluoroborate, was determined by Binks et al.<sup>51</sup> to have an air/IL interfacial tension of 41.7 mN/m. Using this value, we get:

$$(\gamma_{b/w} - \gamma_{b/il}) \approx 0 - 41.7 \cos 64^\circ \approx -18.3 \text{ mN/m} \quad (6)$$

In a similar fashion, for the components of the second term in eq 3, we can write

$$\gamma_{s/w} = \gamma_s - \gamma_w \cos \theta_{s/w} \quad (7)$$

$$\gamma_{s/il} = \gamma_s - \gamma_{il} \cos \theta_{s/il} \quad (8)$$

(50) It should be noted that there is an inherent approximation in this approach: The Young’s equation applies to idealized systems at equilibrium, whereas the measured contact angles are probably not at equilibrium and the experimental surfaces do possess some roughness.

Subtracting eq 8 from eq 7 yields

$$(\gamma_{s/w} - \gamma_{s/il}) = \gamma_{il} \cos \theta_{s/il} - \gamma_w \cos \theta_{s/w} \quad (9)$$

Binks et al.<sup>51</sup> also reported an air–water interfacial tension of 71.9 mN/m and contact angles of < 5° for both  $\theta_{s/w}$  and  $\theta_{s/il}$ . Hence,

$$(\gamma_{s/w} - \gamma_{s/il}) \approx 41.7 - 71.9 \approx -30.2 \text{ mN/m} \quad (10)$$

Substituting in eq 3, we see that the work of separation of bitumen from silica is significantly less (by ~12 mN/m) in an IL than in an aqueous solution. Of course, we have assumed a value for the surface energy of an IL from a similar material, but measurements on a wide range of ILs have shown that their surface tensions lie in the range of 24–53 mN/m, with most clustering in the 40–45 mN/m range.<sup>52</sup>

It can be readily seen that similar arguments would apply to aged crude oil/sand mixtures, because the contact angle between the oil surface and water droplets is ~90°, while the contact angle between the oil surface and the IL used here is ~73° (see Table 1), so that work of separation is again significantly less in ILs than in aqueous solutions.

## Conclusions

The atomic force microscopy (AFM) results presented here clearly show that, at ambient temperatures, the adhesion forces between bitumen and silica are almost an order of magnitude smaller in the ionic liquid (IL) 1-butyl-2,3-dimethyl-imidazolium tetrafluoroborate ([bmmim][BF<sub>4</sub>]) than in an aqueous solution. Although other factors (such as bitumen or oil viscosity) undoubtedly play major roles in the bitumen extraction process, we conclude that this reduction of the force of adhesion must be a major factor in the relative ease of separation observed in ILs. Contact angle measurements reported here also indicate that the work of separation of bitumen from silica is significantly less in an IL than in an aqueous solution. Although AFM measurements could not be made on aged crude oil films directly, thermodynamic arguments also indicate that detachment of oil from silica is much easier in an IL. Finally, the results from the silica-probe/IL/silicon-wafer studies indicate that the formation of ion/charge layers on top of an immersed surface play an important role in the reduction of adhesion forces in the IL, relative to aqueous solutions.

**Acknowledgment.** The authors gratefully acknowledge the support of the National Science Foundation, Polymers Program (under Grant Nos. DMR-0901180 and DMR-1045998).

(51) Binks, B. P.; Dyab, A. K. F.; Fletcher, P. D. I. *Phys. Chem. Chem. Phys.* **2007**, *9*, 6391–6397.

(52) Gardas, R. L.; Coutinho, J. A. P. *Fluid Phase Equilib.* **2008**, *265*, 57–65.